Tetrahedral and Triangular Deformations of $Z = N$ Nuclei in Mass Region $A \sim 60 - 80$

S. Takami, K. Yabana and M. Matsuo*

Graduate School of Science and Technology, Niigata University, Niigata 950-21

** Yukawa Institute for Theoretical Physics, Kyoto University, Kyoto 606-01*

Abstract

We study static non-axial octupole deformations in proton-rich $Z = N$ nuclei, ^{64}Ge, ^{68}Se, ^{72}Kr, ^{76}Sr, ^{80}Zr and ^{84}Mo, by using the Skyrme Hartree-Fock plus BCS calculation with no restrictions on the nuclear shape. The calculation predicts that the oblate ground state in ^{68}Se is extremely soft for the Y_{33} triangular deformation, and that in ^{80}Zr the low-lying local minimum state coexisting with the prolate ground state has the Y_{32} tetrahedral deformation.

PACS numbers: 21.60.Jz, 27.50.+e

Keywords: Skyrme Hartree-Fock, proton-rich Z=N nuclei, non-axial octupole deformation

Spontaneous intrinsic deformation in the ground and excited states is one of the most fundamental properties of nuclei. In addition to the well-established quadrupole deformation, octupole deformation violating reflection symmetries has been attracted much experimental and theoretical attentions. Recently, a pear-shape deformation, i.e., an axially symmetric Y_{30} octupole deformation superposed on a prolate quadrupole deformation has been established in light actinide (Ra-Th isotopes around $A \sim 220$) and lanthanide (Xe-Ba isotopes around $A \sim 136$) mass regions [1]. More exotic shapes such that *violate both reflection and axial symmetries* are known in light p and sd-shell nuclei, where the exotic shapes are caused by α cluster correlations [2], like as the equilateral triangular 3α configuration in ^{12}C. Besides cluster models assuming such configuration, mean-field models [3–5] have also been discussed them in terms of non-axial octupole deformations. It is of great interest to see whether the non-axial exotic octupole deformations realize in heavier systems. Possibilities of the non-axial static octupole deformations have been argued theoretically for superdeformed nuclei [6,7] and for the light Ra region [8], for which however there seem to be no experimental support so far.

Proton-rich nuclei in the $A \sim 60 - 80$ mass region are advantageous candidates for a search of the exotic reflection asymmetric deformations. For nuclei with neutron and proton numbers around 30-40, octupole correlation can be expected because of $\Delta j = 3$ coupling between the $2p_{3/2}$ and $1g_{9/2}$ orbitals in the major pfg-shell [9,10,1]. Furthermore, the shell effect which is the important origin of the deformations is generally large in comparison with those in light lanthanide and actinide nuclei. Especially in proton-rich $Z = N$ nuclei, both proton and neutron configurations coherently operate to develop a static octupole deformation although there is no available experimental information such as $E_x(3^-_1)$ and B(E3) in proton-rich $Z = N$ nuclei around $A \sim 80$, except for ^{64}Ge [11]. The previous theoretical studies based on the shell correction method suggested that the octupole instability is not strong enough [9,11,12] to develop a static octupole deformation in this mass region. However, it should be noted that these models considered only the axially symmetric deformation [9,11], or limited combination of non-axial deformation parameters [12].

In this letter, we will show that the reflection asymmetric shapes violating axial symmetry are more favored in $Z = N$ nuclei in the mass $A = 60 - 80$ region than that with axial symmetry. We perform a fully self-consistent mean-field calculation for even-even nuclei ^{64}Ge, ^{68}Se, ^{72}Kr, ^{76}Sr, ^{80}Zr and ^{84}Mo by means of the Skyrme Hartree-Fock plus BCS method with three-dimensional (3D) mesh representation [13]. In contrast to the previous calculations with 3D mesh representation, we impose no requirement of symmetry on the solutions to allow arbitrary nuclear shapes.

In the present method, quantities such as single-particle wave functions and densities are described on a 3D Cartesian mesh within spherical box. The radius of spherical box and the width of the 3D mesh are set to 12 fm and 1fm, respectively. Imposing the constraints which diagonalize the mass inertia tensor, we make the principal axes coincide with x, y and z axes of the mesh. We adopt the Skyrme III interaction, which has been successful in describing systematically the ground state quadrupole deformation in proton and neutron rich Kr,Sr,Zr and Mo isotopes [13] and in a wide area of nuclear chart [14]. It is also able to describe the axially symmetric octupole deformation in the Ra-Th region [15]. As for the pairing strength of proton, we use the same parameterization $G_p = 16.5/(11 + Z)$ MeV as in Ref. [13] together with the same truncation of the single-particle space. The neutron

pairing strength is taken the same as G_p [16]. To characterize deformation of the obtained solutions, we have calculated the mass multipole moments,

$$\alpha_{lm} \equiv \frac{4\pi\langle\Phi|\sum_i^A r_i^l X_{lm}(i)|\Phi\rangle}{3AR^l}, (m=-l,\cdots,l), \tag{0.1}$$

where A is the number of nucleon and $R = 1.2A^{1/3}$ fm. Here X_{lm} is a real basis of the spherical harmonics,

$$\begin{aligned} X_{l0} &= Y_{l0}, \\ X_{l|m|} &= \frac{1}{\sqrt{2}}(Y_{l-|m|} + Y^*_{l-|m|}), \\ X_{l-|m|} &= \frac{-i}{\sqrt{2}}(Y_{l|m|} - Y^*_{l|m|}), \end{aligned} \tag{0.2}$$

where the quantization axis is chosen as the largest and smallest principal inertia axes for prolate and oblate solutions, respectively. For the quadruple moment, we also use ordinary (β,γ) notation, i.e. , $\alpha_{20} = \beta\cos\gamma, \sqrt{2}\alpha_{22} = \beta\sin\gamma$, mapped in the $\beta > 0, 0 < \gamma < \pi/3$ sections. To represent magnitude of the octupole deformation, we define

$$\beta_3 \equiv (\sum_{m=-3}^{3} \alpha_{3m}^2)^{\frac{1}{2}}, \qquad \beta_{3m} \equiv (\alpha_{3m}^2 + \alpha_{3-m}^2)^{\frac{1}{2}} \qquad (m=0,1,2,3). \tag{0.3}$$

For nuclei around $A \sim 80$, existence of three local energy minimum states showing oblate, nearly spherical and prolate solutions has been reported in the SHF+BCS calculations [13,14]. To search all minimum states close energetically to the ground state, we generate initial states by solving a deformed Wood-Saxon potential model. The five initial states with different quadrupole deformations are used : (1) $\beta = 0.7, \gamma = 60°$, (2) $\beta = 0.3, \gamma = 60°$, (3) $\beta = 0.0, \gamma = 0°$, (4) $\beta = 0.3, \gamma = 0°$, (5) $\beta = 0.7, \gamma = 0°$. For all initial configurations, the octupole distortion, $\alpha_{3m} = 0.1$ $(m = -3,\cdots,3)$, is added.

In table I, we summarize the quadrupole and octupole deformation parameters of the obtained solutions and the excitation energy of the local minimum states, where we do not list states higher than the fourth minimum. The solutions are classified into three groups, oblate, spherical and prolate, according to their quadrupole deformations. As is seen in table I, the calculated quadrupole deformation of the ground states varies significantly as changing the mass number. For $Z = N = 32$ (^{64}Ge), the calculation results in the triaxial deformation, which is in agreement to the experimental indications [11]. It is also seen that the ground state quadrupole deformation changes suddenly from the moderate oblate ones in ^{68}Se and ^{72}Kr to the strong prolate ones in ^{76}Sr and ^{80}Zr. Sudden change of the quadrupole deformation qualitatively agrees with the observed systematics of the first excited energy levels (considered to be $J^\pi = 2^+$ state) from ^{64}Ge to ^{84}Mo [17]. For all the calculated elements, we find the low-lying local minimum states with different quadrupole deformations, which is a characteristic of shape coexistence nuclei.

The octupole deformations violating the axial symmetry are found in the ground state or local minimum states in all nuclei, except ^{64}Ge (where the obtained $\beta_3 = 0.01$ is not sizable). Among them, the second minimum state of ^{80}Zr shows the largest octupole deformation of $\beta_3 = \beta_{32} = 0.24$ without having a quadrupole deformation. The density profile

of this solution shown in Fig. 1 (a) indicates a tetrahedral deformation, which violates the both reflection and axial symmetries, but obeys the symmetry of the point group T_d. Figure 2 (a) shows the potential energy surfaces of ^{80}Zr with respect to the α_{30}, α_{31}, α_{32} and α_{33} deformations, which are calculated under the additional constraints of the mass octupole moments. The potential energy surface of the α_{32} deformation has the minimum point at $\alpha_{32} = 0.24$ which corresponds to the calculated lowest minimum, and the energy gain measured from the spherical solution is as large as 0.71 MeV. This energy gain reduces the energy difference between the spherical and strongly prolate deformed solutions from 1.61 MeV to 0.90 MeV. Octupole instability towards the α_{32} direction (the tetrahedral deformation) is quite contrasting to the other types ($\alpha_{3m}(|m| \neq 2)$) of the octupole deformations.

Instability of the spherical configuration at $Z = N = 40$ for the tetrahedral deformation can be ascribed to the shell effect formed in the potential having the T_d symmetry. In Fig.2 (b), we display the neutron single particle energies as a function of the tetrahedral deformation parameter α_{32}. As developing the tetrahedral α_{32} deformation of ^{80}Zr, the orbitals stemming from $2p_{3/2}$ and $2p_{1/2}$ decrease in energy and those stemming from $1g_{9/2}$ increase with holding high degeneracy of orbitals. The sub-shell gap at nucleon number 40 enhanced by addition of α_{32} distortion field stabilizes the strongly tetrahedral deformed solution. It is known that high degeneracy of irreducible representation of the T_d symmetry tends to produce a significant bunch in the single particle level spectrum as has been demonstrated for electrons in a metallic cluster potential by Hamamoto *et. al.* [18,19]. This tendency exists in nuclear potential with spin-orbit force. Appearance of the tetrahedral deformation due to similar shell effect will not be confined in this neutron/proton number as discussed by Li and Dudek for light actinide isotopes [8]. It is also noted that the tetrahedral octupole deformation competes with the pairing correlation which favors spherical deformation. The energy gain caused by the tetrahedral deformation is found from calculation to be more than 2 MeV when we neglect the pairing. The tetrahedral minimum remains even with 30% increase of the paring strength ($G_p, G_n \sim 0.4$ MeV). It should be mentioned that the measured excitation energies of the fist 3^- levels in Ge and Se isotopes have the minimum points at $N = 40$ [20], which may be a fingerprint of octupole instability.

The other types of non-axial octupole deformation are also found. The ^{68}Se is the most noticeable since it has the large octupole deformation ($\beta_3 = 0.15$) in the ground state. As shown in the density distribution plotted in Fig.1(b), it has Y_{33} triangular distortion superposed on the oblate quadrupole deformation, which obeys the D_{3h} symmetry seen in the regular triangular prism shape. Although the minimum is not as deep as the tetrahedral deformation in ^{80}Zr, the potential energy surface is quite flat up to $\alpha_{33} \sim 0.2$ as shown in Fig.3 (a). It should be noted that octupole instability emerges only for the α_{33} direction. Instability toward the triangular deformation is systematically seen for the excited oblate minima in neighboring ^{72}Kr and ^{76}Sr.

Instability of the oblate states toward the triangular Y_{33} deformation can also be related to the single-particle shell structure formed in the oblate deformed potential. Figure 4 shows the neutron Nilsson diagram as a function of quadrupole deformation obtained in the constrained SHF+BCS method, in which axial and reflection symmetries are imposed. In the oblate configuration of ^{68}Se, the $N, Z = 34$ Fermi surfaces are located between the positive parity orbitals with $\Omega = 9/2, 7/2, ..., 1/2$ stemming from the $1g_{9/2}$ and the negative parity orbitals with $\Omega = 3/2, 1/2$ arising from the $2p_{3/2}$ (those just below the Fermi surface,

See Fig.4). Among the possible couplings associated with the octupole deformations, the $\Delta\Omega = 3$ coupling between the positive parity $\Omega = 9/2$ and negative parity $\Omega = 3/2$ orbitals, and also the one between the positive parity $\Omega = 7/2$ and negative parity $\Omega = 1/2$ orbitals have the smallest energy difference, and give enhanced softness toward the triangular Y_{33} deformation.

In the prolate solutions of ^{68}Se and ^{72}Kr, the non-axial octupole deformations with finite value of β_{31} (so-called 'banana' shape) are also found although the magnitude of the deformation is small. The associated potential energy surface for the octupole deformations, shown in Fig.3.(b), indicates that the α_{31} direction is soft while the other types including α_{30} pear-like deformation are not. It is noted that the positive parity orbital with $\Omega = 3/2$ (stemming from $1g_{9/2}$) and the negative parity $\Omega = 1/2$ ($2p_{3/2}1f_{1/2}$) located near the $N, Z = 34 - 36$ Fermi surface (see Fig.4) are responsible for the Y_{31} deformation. Although there exists closely-lying $\Delta\Omega = 0$ pair of $\Omega = 1/2$ ($1g_{9/2}$) and $\Omega = 1/2$ ($2p_{3/2}1f_{1/2}$) orbitals, the matrix element of the $\Delta\Omega = 0$ octupole operator r^3Y_{30} between these orbitals is expected to be small, provided these orbitals have good asymptotic Nilsson $[440]\frac{1}{2}$ and $[310]\frac{1}{2}$ components, respectively.

In summary, the self-consistent mean-field calculation predicts that ^{80}Zr has the low-lying coexisting state showing the spontaneous Y_{32} tetrahedral deformation and the oblate ground state in ^{68}Se is extremely soft with respect to the Y_{33} triangular deformation. Appearances of the non-axial octupole deformations are governed by the single-particle shell structures at $N, Z \sim 40$ and $N, Z \sim 34$ for the tetrahedral and triangular deformations, respectively.

The non-axial octupole deformations discussed above will accompany specific spectroscopic properties of excited states. The intrinsic tetrahedron shape having the T_d symmetry leads to a series of levels with $I^\pi = 0^+, 3^-, 4^+, 6^+, 7^-, \cdots$, which follow the $E(I) - E(0) \sim I(I+1)$ relation and are connected with strongly enhanced E3 transitions [5]. In ^{80}Zr, for example, a low-lying excited $J^\pi = 3^-$ state is expected, and one could observe a strong E3 decay from a 3^- state to a low-lying 0^+ state associated with the tetrahedral deformed second minimum. The oblate deformed ground state of ^{68}Se which is extremely soft towards the Y_{33} direction will accompany a low-lying 3^- excited state with high collectivity. Furthermore, the intrinsic triangular shape having the D_{3h} symmetry may form the characteristic band structure, that is, the ground band $I^+ = 0^+, 2^+, 4^+, \cdots$ and a $K^\pi = 3^-$ band $I^- = 3^-, 4^-, 5^-, \cdots$ as seen in ^{12}C [2].

The authors would like to thank Prof. K. Matsuyanagi for helpful discussions. Numerical computation in this work was mainly performed at the Yukawa Institute Computer Facility. Part of numerical calculations were also performed on the FACOM VPP-500 supercomputer in RIKEN.

REFERENCES

[1] As a review, P. A. Butler and W. Nazarewicz, *Rev. Mod. Phys.* **68**(1996)349.

[2] As a review, Y. Fujiwara, H. Horiuchi, K. Ikeda, M. Kamimura, K. Katō, Y. Suzuki and E. Uegaki, *Prog. Theor. Phys. Suppl.* **68**(1980)29.
H. Horiuchi and K. Ikeda, in *International Review of Nuclear Physics*, ed. T. T. S. Kuo and E. Osnes (World Scientific, Singapore, 1986), Vol. 4, p. 1.

[3] J. Eichler and A. Faessler, *Nucl. Phys.* **A157**(1970)166.

[4] G. Leander and S. E. Larsson, *Nucl. Phys.* **A239**(1975)93.

[5] J. P. Elliott, J. A. Evans and E. E. Maqueda, *Nucl. Phys.* **A437**(1985)208.

[6] X. Li, J. Dudek, and P. Romain, *Phys. Lett.***B271**(1991)281.

[7] R. R. Chasman, *Phys. Lett.* **B266**(1991)243.

[8] X. Li and J. Dudek, *Phys. Rev.* **C94**(1994)R1250.

[9] W. Nazarewicz, P. Olanders, I. Ragnarsson, J. Dudek, G. A. Leander, P. Mőller and E. Ruchowska, *Nucl. Phys.* **A429**(1984)269.

[10] G. A. Leander, R. K. Sheline, P. Mőller, P. Olanders, I. Ragnarsson and A. J. Sierk, *Nucl. Phys.* **A388**(1982)452.

[11] P. J. Ennis, C. J. Lister, W. Gelletly, H. G. Price, B. J. Varley, P. A. Butler, T. Hoare, S. Cwiok and W. Nazarewicz, *Nucl. Phys.* **A535**(1991)392.

[12] J. Skalski, *Phys. Rev.* **C43**(1991)140.

[13] P. Bonche, H. Flocard, P.-H. Heenen, S. J. Krieger and M. S. Weiss, *Nucl. Phys.* **A443**(1985)39.

[14] N. Tajima, S. Takahara and N. Onishi, *Nucl. Phys.* **A603**(1996)23.

[15] P. Bonche, P. H. Heenen, H. Flocard and D. Vautherin, *Phys. Lett.* **B175**(1986)387.

[16] P.-H.Heenen, J.Skalski, P. Bonche, and H. Flocard, *Phys. Rev.* **C50**(1994)802.

[17] C.J.Lister,M.Campbell,A.A.Chishti,W.Gelletly,L.Goettig,R.Moscrop, B.J.Vary,A.N.James, T.Morrison, H.G.Price,J.Simpson,K.Connel, and O.Skeppstedt, *Phys. Rev. Lett.* **59**(1987)1270.
B.J.Vary, M.Campbell, A.A.Chishti, W.Gelletly, L.Goettig, C.J.Lister, A.N.James, and O.Skeppstedt, *Phys. Lett.* **B194**(1987)463.
H.Dejbakhsh, T.M.Cormier, X.Zhao, A.V.Ramayya, L.Chaturvedi, S.Zhu, J. Kormicki,*Phys. Lett.* **B249**(1990)195.
J.H.Hamilton,M.Satteson,I.Y.Lee,C.Baktash,F.K.McGowan,N.R.Johnson, J.D.Cole, and E.F.Zganjar, C. J. Lister, P. J. Ennis, A. A. Chishti, B. J. Varley, W. Gelletly, H. G. Price and A. N. James, *Phys. Rev.* **C42**(1990)R1191.
W. Gelletly, *et. al.*, *Phys. Lett.* **B253**(1991)287.

[18] I. Hamamoto, B. Mottelson, H. Xie and X. Z. Zhang, *Z. Phys.* **D21**(1991)163.

[19] F. Frisk, I. Hamamoto and F. R. May, *Phys. Scr.* **50**(1994)628.

[20] P.D. Cottle, *Phys. Rev.* **C42**(1990)1264.

FIGURES

FIG. 1. Density distributions of proton in the xy, yz and zx planes where x, y and z axes represent the principal inertia axes. (a) and (b) show those of the second minimum state of ^{80}Zr and the ground state of ^{68}Se, respectively.

FIG. 2. (a) The potential energy surfaces of ^{80}Zr with respect to the different types of the octupole deformations, where the energy is measured in relative to the spherical solution. The potential energy is calculated as a function of α_{3m} ($m = 0, 1, 2, 3$) by imposing the constraints of $\beta = 0, \gamma = 0^\circ$ and $\alpha_{3\nu} = 0$ ($\nu \neq m$). (b) The single particle energy of neutron as a function of the tetrahedral α_{32} deformation.

FIG. 3. Potential energy surfaces with respect to the different types of octupole deformations, calculated for the oblate ground state (a) and the second minimum prolate state (b) of ^{68}Se. The quadrupole deformations are set to $\beta = 0.25, \gamma = 60^\circ$ and $\beta = 0.25, \gamma = 0^\circ$ for the ground and second minimum states, respectively.

FIG. 4. The neutron single-particle levels for ^{80}Zr as a function of the quadrupole deformation parameter β_2 calculated with the quadrupole constraint and the axial and reflection symmetries. For each orbitals, we put the value of Ω, the projection of the angular momentum along the symmetry axis. The arrows indicate the $\Delta\Omega = 3$ coupling associated with the triangular Y_{33} deformation as discussed in the text.

TABLES

	Oblate		Spherical	Prolate	
^{64}Ge		g.s.		0.62	4.00
		$\beta, \gamma = 0.27, 25^\circ$ (T)		$\beta, \gamma = 0.24, 6^\circ$	$\beta, \gamma = 0.38, 0^\circ$
		$\beta_3 = \beta_{33} = 0.01$		$\beta_3 = 0.00$	$\beta_3 = 0.00$
^{68}Se		g.s.		0.32	2.42
		$\beta, \gamma = 0.25, 60^\circ$		$\beta, \gamma = 0.25, 0^\circ$	$\beta, \gamma = 0.40, 18^\circ$ (T)
		$\beta_3 = \beta_{33} = 0.15$		$\beta_3 = \beta_{31} = 0.06$	$\beta_3 = \beta_{31} = 0.02$
^{72}Kr	g.s.	1.12		1.74	
	$\beta, \gamma = 0.34, 60^\circ$	$\beta, \gamma = 0.27, 58^\circ$		$\beta, \gamma = 0.42, 1^\circ$	
	$\beta_3 = 0.00$	$\beta_3 = \beta_{33} = 0.05$		$\beta_3 = \beta_{31} = 0.03$	
^{76}Sr		2.58	3.25		g.s.
		$\beta, \gamma = 0.13, 60^\circ$	$\beta, \gamma = 0.02, 0^\circ$		$\beta, \gamma = 0.49, 0^\circ$
		$\beta_3 = \beta_{33} = 0.16$	$\beta_3 = \beta_{32} = 0.12$		$\beta_3 = 0.00$
^{80}Zr		1.58	0.90		g.s.
		$\beta, \gamma = 0.20, 59^\circ$	$\beta, \gamma = 0.00, 0^\circ$		$\beta, \gamma = 0.50, 0^\circ$
		$\beta_3 = \beta_{32} = 0.04$	$\beta_3 = \beta_{32} = 0.24$		$\beta_3 = 0.00$
^{84}Mo		g.s.	0.24		0.85
		$\beta, \gamma = 0.20, 56^\circ$	$\beta, \gamma = 0.05, 60^\circ$		$\beta, \gamma = 0.64, 0^\circ$
		$\beta_3 = 0.00$	$\beta_3 = \beta_{30} = 0.13$		$\beta_3 = 0.00$

TABLE I. The ground states and the local minimum states obtained in the present SHF+BCS calculation. The energy difference (MeV) between the ground state and the local minimum state (the ground state is denoted as g.s.), the quadrupole and octupole deformation parameters are shown, where label (T) stands for the triaxial deformation. For the solutions showing the octupole deformation, the most dominant component of β_{3m} is also presented. Each solutions are classified into the three groups, oblate, spherical and prolate by their quadrupole deformation parameter, except for the ground state of ^{64}Ge. The ground state of ^{64}Ge which shows the triaxial deformation is classified into the oblate group.

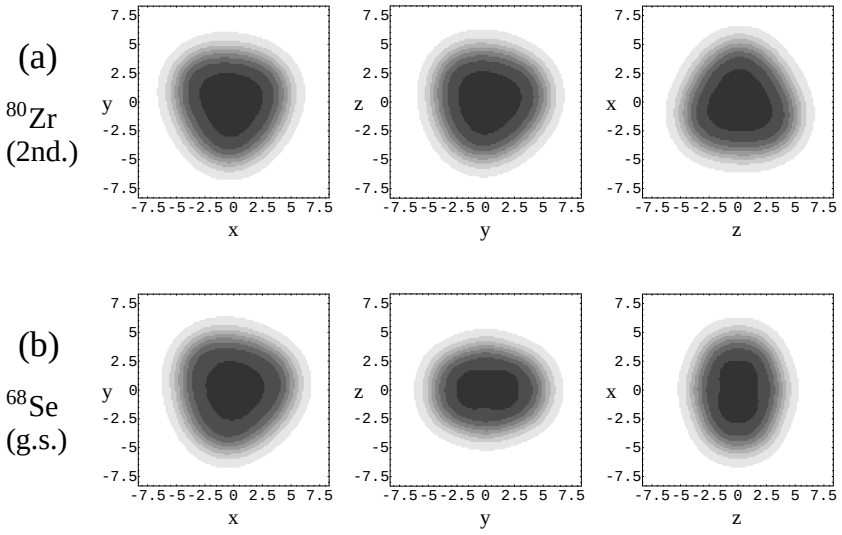

Figure 1

(a)

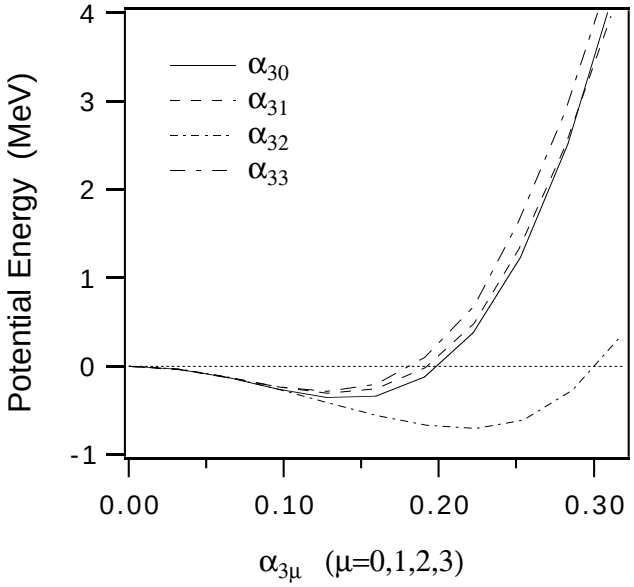
Potential Energy (MeV)
4
3
2
1
0
-1
0.00
0.10
0.20
0.30
α_{30}
α_{31}
α_{32}
α_{33}
$\alpha_{3\mu}$ (μ=0,1,2,3)

(b)

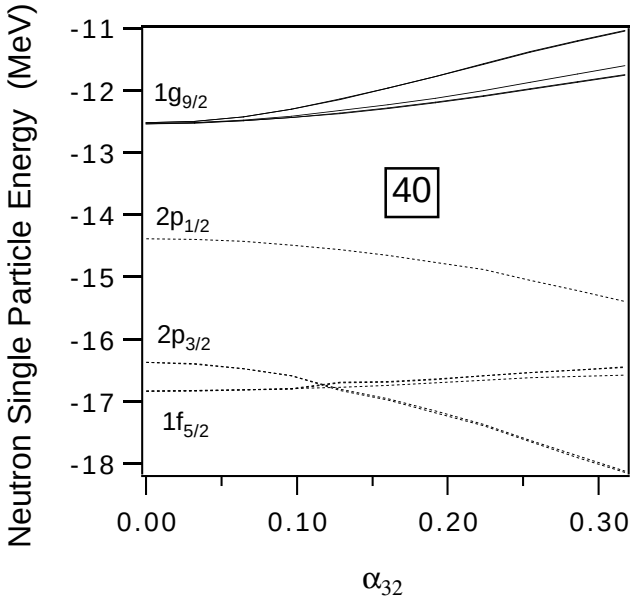
Neutron Single Particle Energy (MeV)
-11
-12
-13
-14
-15
-16
-17
-18
0.00
0.10
0.20
0.30
$1g_{9/2}$
40
$2p_{1/2}$
$2p_{3/2}$
$1f_{5/2}$
α_{32}

Figure 2

(a)

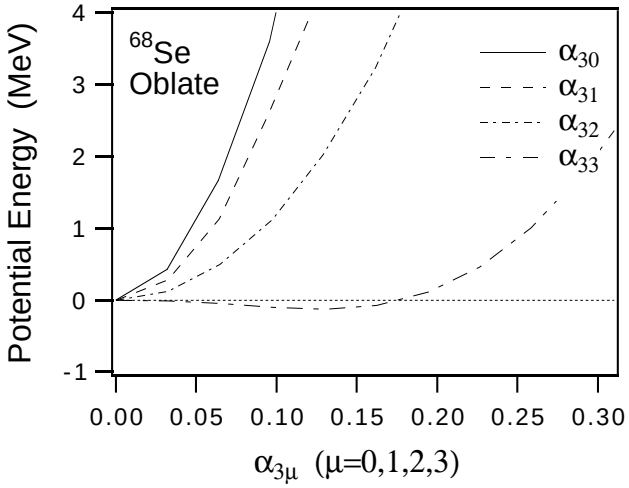
^{68}Se
Oblate
α_{30}
α_{31}
α_{32}
α_{33}
Potential Energy (MeV)
4
3
2
1
0
-1
0.00
0.05
0.10
0.15
0.20
0.25
0.30
$\alpha_{3\mu}$ (μ=0,1,2,3)

(b)

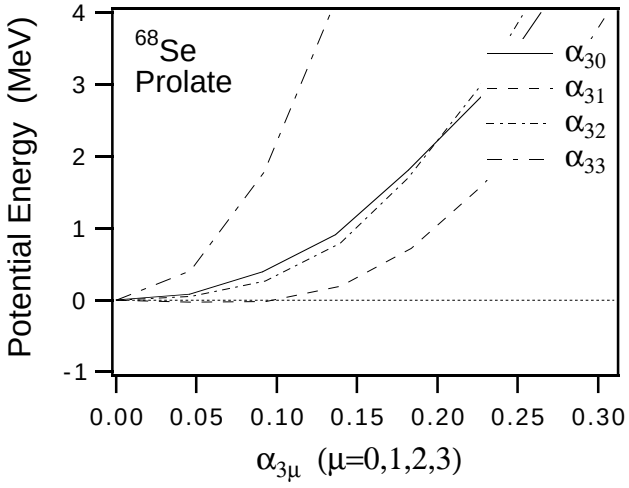
^{68}Se
Prolate
α_{30}
α_{31}
α_{32}
α_{33}
Potential Energy (MeV)
4
3
2
1
0
-1
0.00
0.05
0.10
0.15
0.20
0.25
0.30
$\alpha_{3\mu}$ (μ=0,1,2,3)

Figure 3

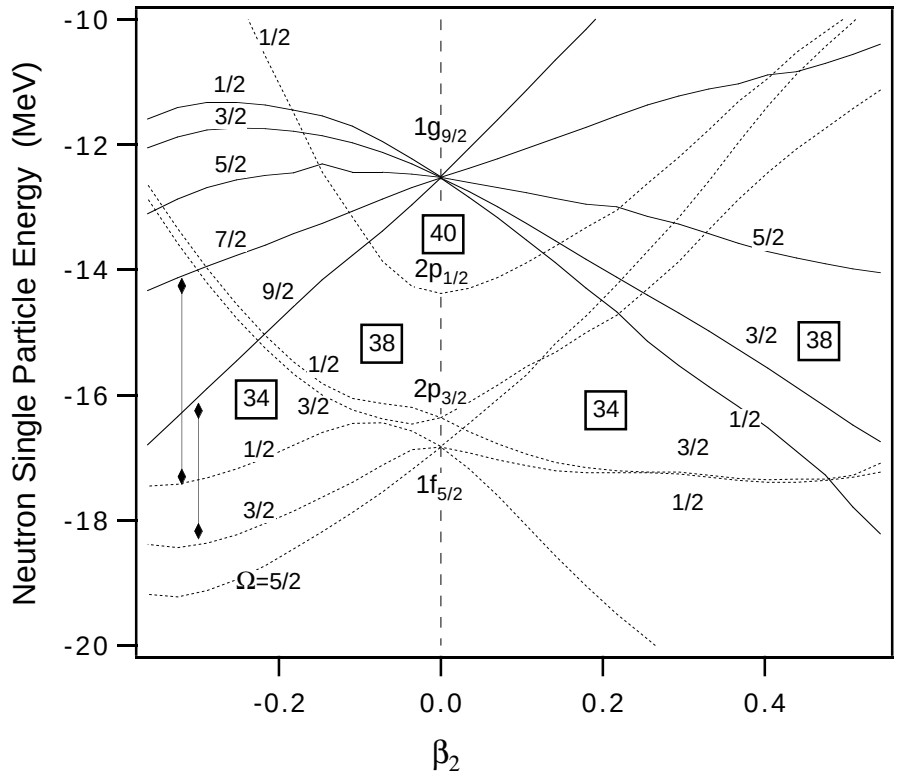
Neutron Single Particle Energy (MeV)
-10
-12
-14
-16
-18
-20
-0.2
0.0
0.2
0.4
β2
1/2
1/2
3/2
5/2
7/2
9/2
1g9/2
40
2p1/2
38
34
2p3/2
1f5/2
Ω=5/2

Figure 4